Anisotropy effect on global minimum structures of clusters: Two-center Lennard-Jones model

Yan Feng, Jing Wu, Longjiu Cheng, and Haiyan Liu

Citation: J. Chem. Phys. **135**, 244108 (2011); doi: 10.1063/1.3672237
View online: http://dx.doi.org/10.1063/1.3672237
View Table of Contents: http://jcp.aip.org/resource/1/JCPSA6/v135/i24
Published by the American Institute of Physics.

Anisotropy effect on global minimum structures of clusters: Two-center Lennard-Jones model

Yan Feng,[1,2,a)] Jing Wu,[2] Longjiu Cheng,[2,b)] and Haiyan Liu[1]
[1]*Hefei National Laboratory for Physical Sciences at the Microscale, and School of Life Sciences, University of Science and Technology of China, Hefei, Anhui 230026, China*
[2]*School of Chemistry and Chemical Engineering, Anhui University, Hefei, Anhui 230039, China*

(Received 19 October 2011; accepted 6 December 2011; published online 29 December 2011)

Using a two-center Lennard-Jones (2CLJ) model, the simplest anisotropic case, we investigated how anisotropy affects global minimum structures of clusters and obtained some interesting results. The anisotropy parameter, R, is defined as the ratio of the bond length of 2CLJ dimer to the LJ equilibrium pair separation, where a larger R value means higher anisotropy. For low R values, the structures resemble those of the Lennard-Jones atomic clusters. However, as the pairwise interaction becomes more anisotropic, the "magic numbers" change, and several novel cluster patterns emerge as particularly stable structures, and the global minima change from icosahedral, to polyicosahedral and to novel irregular structures. Moreover, increasing the anisotropy effectively softens the 2CLJ potential. Given the general importance of the LJ cluster as a simple model cluster, 2CLJ model can provide a straightforward and useful analysis of the effect of molecular shape on the structures of clusters. [doi:10.1063/1.3672237]

I. INTRODUCTION

The properties evolving between isolated atoms and condensed materials are of increasing interest.[1] As a bridge between isolated atoms/molecules and bulk material, the atomic or molecular clusters play a very important role in understanding the microstructures of the materials. Some nanoclusters are expected to be widely employed in innovative technology, as they range from industrial catalysis to the miniaturization of electronic devices.[2,3] Because of the cost of computation for global geometric optimization of large clusters, model, and empirical potentials are often used to fit the interactions among particles.

The Lennard-Jones (LJ) potential, as a benchmark system, is often used to simulate atomic clusters, especially for rare gas atomic clusters.[4–8] It also plays an important role in studying the nonbonding pair interactions in many complex molecular systems. The LJ pair potential[6] can be written as

$$E_{\mathrm{LJ}}(r) = \varepsilon\left[\left(\frac{r_0}{r_{ij}}\right)^{12} - 2\left(\frac{r_0}{r_{ij}}\right)^{6}\right], \qquad (1)$$

where r_0 denotes the equilibrium pair separation between two atoms, ε is the pair well depth, and the reduced units ($r_0 = \varepsilon = 1$) are often used for model study. The LJ model is obviously simple to implement, and their optimal structures display a very regular variation. For LJ clusters, icosahedral motifs are most favored, and only at some magic numbers, decahedral, face-centered cubic (fcc), and tetrahedral motifs can be global minima. For example, LJ_{38} is fcc; $LJ_{75–77}$ and $LJ_{102–104}$ are decahedral; and LJ_{98} is tetrahedral.[9] Binary Lennard-Jones model potential is also used to study heterogeneous alloy.[10,11] The magic numbers in binary Lennard-Jones clusters[12] are polyicosahedral clusters. For C_{60} molecular clusters with all-atom potential,[13] the intermolecular interaction between C_{60} molecules is nearly the sum of C–C LJ interactions between two molecules. This kind of C_{60}–C_{60} interaction is somewhat a multi-center LJ model where realistic molecular anisotropy is considered. Their favorite structures are much different from those of the LJ potential, where decahedral and close-packed motifs are more favored for C_{60} molecular clusters.[14,15]

Herein, the simplest case of an anisotropy two-center Lennard-Jones (2CLJ) dimer is modeled, where each dimer consists of two LJ atoms and only the LJ interactions between different dimers are considered. Given the general importance of the LJ cluster as a simple model cluster, 2CLJ model can provide a straightforward analysis of the effect of molecular shape on the structures of clusters. The anisotropy parameter R is defined as the ratio of the bond length of 2CLJ dimer to the LJ equilibrium pair separation. R is varied to increase the degree of anisotropy. Large R means strong anisotropy effect. This model guarantees an anisotropic interaction of clusters as well as the low computational cost. Different from LJ clusters, the 2CLJ dimer is anisotropy, so there must be some interesting lowest energy structures with the increase of anisotropy effect. The global minima of 2CLJ clusters are investigated for a range of value R from 0.1 to 0.8 (step size is 0.1). Meanwhile, anisotropy effect of the 2CLJ dimer on the potential range is also discussed. The potential energy surface of 2CLJ clusters is more rugged than that of LJ clusters, so the highly efficient "funnel hopping" algorithm[16] is employed to carry out this searching on the potential energy surfaces.

II. METHODS

Two-center Lennard-Jones model is important in physics.[17] In this work, as a model study and for simplicity,

a)Electronic mail: fy@ustc.edu.
b)Electronic mail: clj@ustc.edu.

each molecule is taken as a rigid body and only the LJ interactions are considered. The LJ potential is described in the reduced unit. Then, using the 2CLJ model, the energy between two molecules can be written as

$$E(\alpha, \beta) = \sum_{i=1}^{2} \sum_{j=1}^{2} E_{\mathrm{LJ}}\left(r_{ij}^{\alpha\beta}\right), \tag{2}$$

where $r_{ij}^{\alpha\beta}$ is the distance between atom i of molecule α and atom j of molecule β. As a result, the structure of $2CLJ_2$ is determined by the diatomic bond length and the LJ equilibrium length.

In this work, "funnel hopping" algorithm[16], an unbiased global optimization tool, is used to locate the global minimum structures of the 2CLJ clusters. The basic idea of this algorithm is to insert a second local optimization (LO)-phase between the first gradient-based LO-phase and the global optimization (GO)-phase. The goal of the second LO-phase is to locate the minimum of the funnel that contains current configuration in the energy landscape with the least cost. Then the GO-phase can focus on the global information of the potential energy surface over the various funnels. The first LO-phase is the limited memory quasi-Newton method,[18] the second LO-phase is a funnel optimizer by cluster surface smoothing (CSS) and the GO-phase is a simple version of genetic algorithm (GA) (Refs. 19–21). CSS method is similar to the dynamic lattice searching method,[22] which can smooth the cluster surface by optimizing the approximate lattice. This "funnel hopping" approach has been proved to be useful for structure optimization of atomic and molecular clusters.

At a small R, the anisotropy effect of 2CLJ is small, and the potential energy surface is relatively flat. At $R = 0.1$ and 0.2, we obtained the putative global minimum structures up to $N = 80$. For each cluster size, 10 separate runs are performed, and for each run 1000 hoppings are carried out. In the 10 separate runs, the same putative global minima are located by 8–10 times, which indicates high reliability of our global optimization results. With R increasing, the anisotropy effect also increases, so the global optimization becomes difficult. At $R = 0.3$, we only optimize the structures up to $N = 61$, and the number of hitting the putative global minimum is 3–5 out of 10 runs at large N. At $R = 0.4$–0.8, it is increasingly difficult to optimize the structures, so we only obtained the global minimum structures up to $N = 30$. For each cluster size, we carry out 50 separate runs. The probabilities of hitting the global minima are only 3–10/50 in the 50 separate runs for large cluster sizes. With R increasing, the probabilities of finding the global minima decrease as the potential energy surface becomes more rugged. At $N = 30$ and $R = 0.8$, the putative global minimum is located for only 3 times in the 50 runs, and the other minima are also located for only 1–3 times. The other minima may be close to the global minimum one in energy, but their structures are irregular and very different to each other.

III. RESULTS AND DISCUSSION

We have located the global minima for 2CLJ clusters at different R. At small R (0.1, 0.2, and 0.3), the structures of 2CLJ clusters are regular and comparable to those of LJ clusters, so they are discussed in Sec. III A. For $R = 0.4$–0.8, the structures are very irregular and novel, so they are discussed in Sec. III B. Anisotropy effect of 2CLJ dimer on the range of 2CLJ pair potential is discussed in Sec. III C.

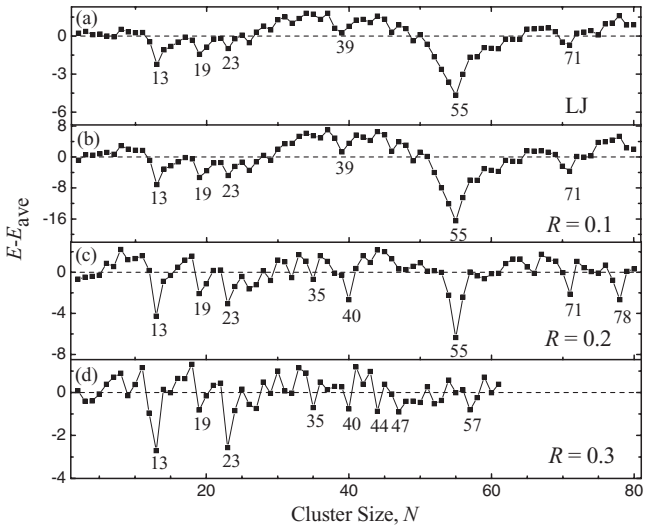

FIG. 1. Plots of the relative energy of the global minima as a function of cluster size $2 \le N \le 80$ with the LJ and 2CLJ potential at $R = 0.1$, 0.2, and 0.3. E is the energy of the global minima, and E_{ave} is a four-parameter fit to the global minima energy ($E_{\mathrm{ave}} = aN + bN^{2/3} + cN^{1/3} + d$). Downward peaks represent the most stable magic numbers compared to the neighbors. Data of LJ clusters are from the Cambridge Cluster Database.[23]

A. Structures of 2CLJ clusters at $R = 0.1$, 0.2, and 0.3

Figure 1 plots the energy sequences of the global minima of LJ (Ref. 23) and 2CLJ potentials at $R = 0.1$, 0.2, and 0.3 in a manner that emphasizes particular stable minima or "magic numbers." At $R = 0.3$, we have only located the optimal structures up to 61 due to the rugged potential energy surface. At $R = 0.1$ (Fig. 1(b)), the most stable structures are still icosahedral ($N = 13$, 19, 23, 39, 55, and 71), which is the same as those of LJ clusters (Fig. 1(a)). The energy sequences of LJ and 2CLJ at $R = 0.1$ have very similar outlines, which demonstrates that they favor similar structures and the anisotropy effect on structure is very weak at $R = 0.1$. In Fig. 1(c), at $R = 0.2$, some new magic numbers ($N = 35$, 40, and 78) with polyicosahedral structures are viewed, but the peak of magic number at $N = 39$ with icosahedral structure disappears. The energy sequence at $R = 0.3$ in Fig. 1(d) has similar outline with that in Fig. 1(c). The difference is that in Fig. 1(d), the peaks of the polyicosahedral magic number ($N = 44$, 47, and 57) appear, while the icosahedral magic number ($N = 55$) disappears. In fact, with R increasing, peaks of some icosahedral magic numbers gradually disappear, such as 55, but many polyicosahedral magic numbers emerge.

Figure 2 plots the magic number and typical structures of 2CLJ clusters ($R = 0.1$, 0.2, and 0.3), and for comparison, the structures of LJ clusters are also given. As shown in Fig. 2(a), LJ_{13}, LJ_{39}, and LJ_{55} are regular Mackay icosahedra (Ih13, Ih39, and Ih55); LJ_{19} and LJ_{23} are Ih13 plus various regular anti-Mackay overlayers; LJ_{71} is Ih55 plus a cap with

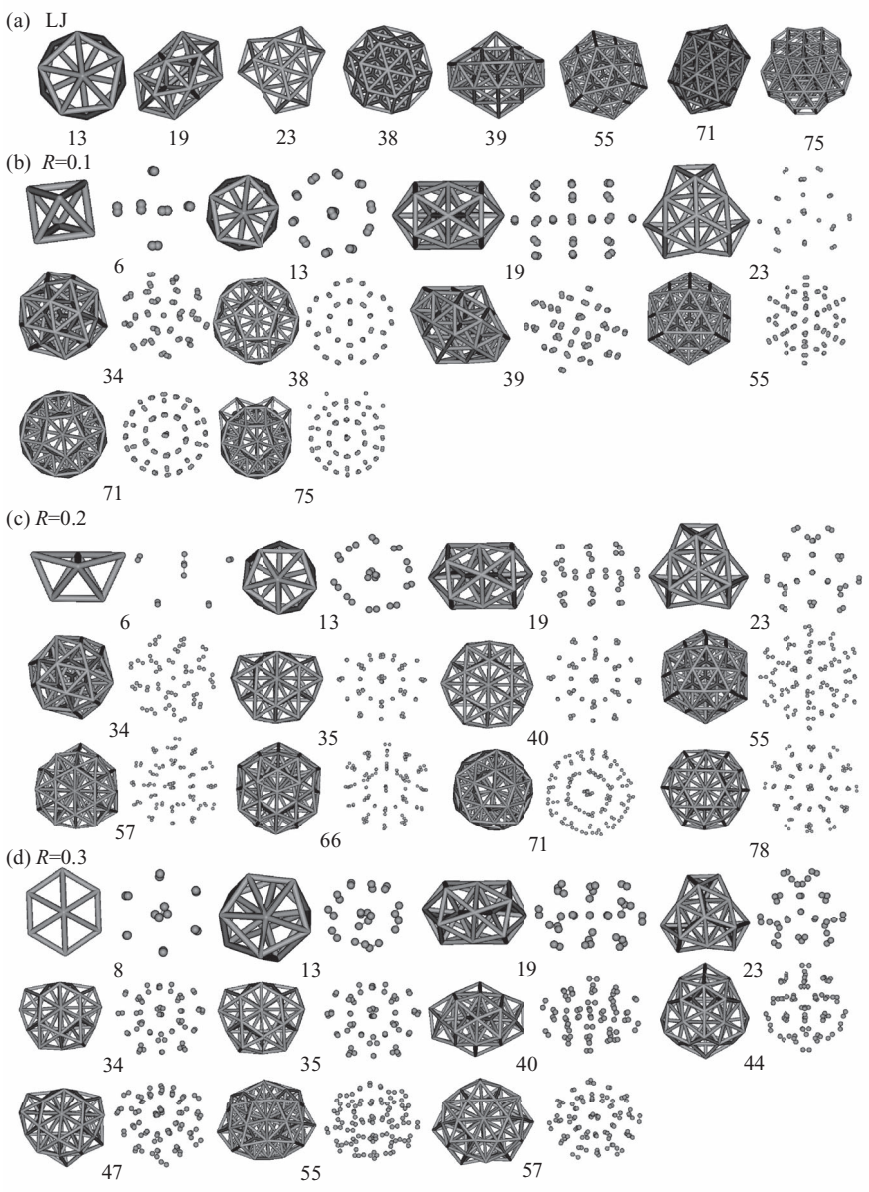

FIG. 2. Global minima of LJ and 2CLJ molecular clusters at $R = 0.1$, 0.2, and 0.3. For each cluster size, the structure on the left shows an overall view of the cluster (each ball means the mass center of each dimer) and that on the right shows the real diatomic orientations in the diatomic molecule.

anti-Mackay overlayers; LJ_{38} is fcc truncated octahedron; and $LJ_{75–77}$ are decahedra.

Figure 2(b) plots the magic number and typical structures of 2CLJ clusters at $R = 0.1$. Compared to LJ clusters, $2CLJ_{13}$, $2CLJ_{19}$, $2CLJ_{23}$, $2CLJ_{39}$, $2CLJ_{55}$, and $2CLJ_{71}$ are still icosahedral magic numbers. However, the fcc and decahedral structures are not global minima any longer, and $2CLJ_{38}$ and $2CLJ_{75–77}$ become icosahedral too. More interestingly, $2CLJ_{34}$ is a distorted Leary tetrahedral motif with T symmetry, whose packing style is similar to Leary tetrahedral LJ_{98}.[24]

Figure 2(c) plots the magic number and typical structures of 2CLJ clusters at $R = 0.2$. $2CLJ_{13}$, $2CLJ_{19}$, $2CLJ_{23}$, $2CLJ_{55}$, and $2CLJ_{71}$ are still icosahedral (may be distorted). However, the anti-Mackay cap of $2CLJ_{71}$ is distorted to have more nearest neighbors, where similar distortion is viewed in the Morse clusters.[25] $2CLJ_{34}$ is still a Leary tetrahedral structure. $2CLJ_{40}$ is a novel polyicosahedral structure in a six-fold manner, which is also the global minimum structure of modified Morse clusters.[26] Similarly, $2CLJ_{35}$, $2CLJ_{57}$, $2CLJ_{66}$, and $2CLJ_{78}$ are also polyicosahedral structures.

Figure 2(d) plots the magic number and typical structures of 2CLJ clusters at $R = 0.3$. $2CLJ_8$ becomes a novel structure in a six-fold manner. $2CLJ_{13}$, $2CLJ_{19}$, and $2CLJ_{23}$ are still icosahedral but seriously distorted. $2CLJ_{34}$ changes from Leary tetrahedron to polyicosahedron. $2CLJ_{35}$, $2CLJ_{40}$, $2CLJ_{44}$, $2CLJ_{47}$, and $2CLJ_{57}$ are polyicosahedral. $2CLJ_{55}$ now changes from icosahedron to polyicosahedron.

To give an overview of the structural transition for 2CLJ clusters at different R, the distributions of global minimum structures for LJ and 2CLJ clusters are given in Table I. It can be seen that, from LJ to 2CLJ with $R = 0.1$, the decahedral and fcc structures (LJ_{38}, $LJ_{75–77}$) disappear. The strain energy and nearest neighbor energy contribute largely to the total energy of the atomic clusters,[27] so does it in the diatomic

TABLE I. Distributions of the global minimum structures for LJ and 2CLJ clusters at $13 \leq N \leq 80$.

Clusters	Icosahedral	Polyicosahedral	Else
LJ	13–37, 39–74,78–80		38, 75–77
2CLJ ($R = 0.1$)	13–33, 35–80		34
2CLJ ($R = 0.2$)	13–31, 54–56, 70–72	32, 33, 35–53, 57–69, 73–80	34
2CLJ ($R = 0.3$)	13–31	32–61	

clusters. In atomic clusters, compared to icosahedral motif, decahedral and fcc motifs have less nearest neighbor numbers but are less strained. However, for the 2CLJ model, the fcc structures are not strain-free any more because of the diatomic anisotropy, so the less-strained structures become disfavored in energy. The six-fold polyicosahedral motifs are too strained for LJ clusters. However, for 2CLJ clusters at large R, all packings (icosahedral, decahedral, and polyicosahedral) are seriously strained, so the six-fold polyicosahedral packing is favored due to its large number of nearest neighbors. This kind of polyicosahedral packing is also favored for binary LJ clusters[12] at certain size rang.

B. Structures of 2CLJ clusters at $R = 0.4$–0.8

The global minima and magic numbers of 2CLJ clusters with size $N \leq 30$ at $R = 0.4$–0.8 are located. Compared with LJ and 2CLJ at $R = 0.1$–0.3 whose global minimum structures are regular, with the increase of anisotropy effect, the structures of 2CLJ clusters are various and novel, some of which are interesting.

To find out the most stable magic numbers at the different R, the energy sequences of the global minima at $R = 0.4$–0.8 are plotted in Fig. 3. It is seen that at $R = 0.4$, the magic number is 9, 12, and 23; at $R = 0.5$, the magic number is 8, 12, and 29; at $R = 0.6$, the magic number is 8, 11, and 16; at $R = 0.7$, the magic number is 8, 11, 15, 18, 27, and 30; at $R = 0.8$, the magic number is 8, 11, 13, 16, and 27. With the cluster size increasing, most of the magic numbers are the structures with one or two diatomic molecules in the center and others surrounding them to have more nearest neighbors.

Figure 4 plots the magic number and typical structures of 2CLJ clusters at $R = 0.4$–0.8. Figure 4(a) shows the magic number and some typical structures of global minima at $R = 0.4$. At small size, the 2CLJ molecules try to arrange themselves parallel or perpendicular to each other. As is shown in Fig. 4(a), two molecules in $2CLJ_2$ are perpendicular to each other. Three molecules in $2CLJ_3$ are parallel to each other, where the mass centers are in regular triangle. $2CLJ_4$ is a trigonal pyramid motif. $2CLJ_5$ and $2CLJ_6$ are based on trigonal bipyramid motif. $2CLJ_7$ is a decahedron where two molecules at top and bottom are perpendicular to each other. $2CLJ_8$ and $2CLJ_9$ are similar, where seven molecules are paralleled to form a bottom plus a vertex, and $2CLJ_9$ is a particular stable structure. $2CLJ_{11-13}$ is the structure with one molecule in the center and the others surrounding them, which can make the clusters more compact to have more nearest

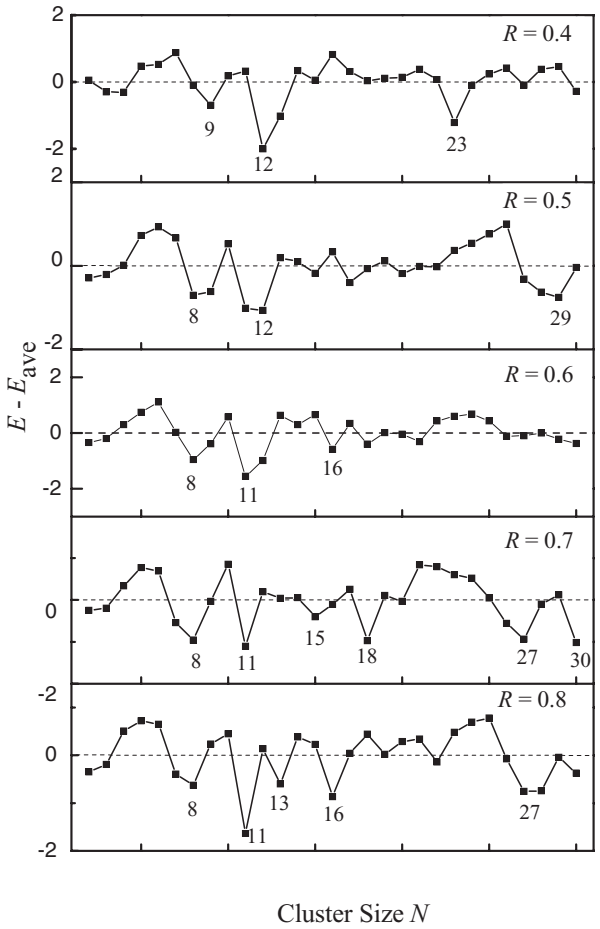

FIG. 3. Plots of the relative energy of the global minima as a function of cluster size ($N \leq 30$) at (a) $R = 0.4$, (b) $R = 0.5$, (c) $R = 0.6$, (d) $R = 0.7$, and (e) $R = 0.8$.

neighbors. $2CLJ_{23}$ is also a compact structure but with two molecules in the center.

Figure 4(b) shows the magic number and some typical global minimum structures at $R = 0.5$. The structure of $2CLJ_8$ is similar with that at $R = 0.4$, but it becomes a magic number structure now. $2CLJ_9$ is an interesting structure with C_2 symmetry, just like a windmill with three sails at 90° angle, while $2CLJ_{11}$ is like a windmill with four sails and with D_2 symmetry. In this windmill structure, one sail is made of two 2CLJ dimers and the dimers at windmill center are paralleled in a shoulder-to-shoulder manner. $2CLJ_{12}$, $2CLJ_{13}$, and $2CLJ_{16}$ are the structures with one molecule in the center and the others surrounding them, and $2CLJ_{12}$ is a particular stable structure. $2CLJ_{14}$ and $2CLJ_{15}$ are with C_{2v} and C_2 symmetry, respectively, and their structural motifs are also very novel. $2CLJ_{29}$ is also a particular stable structure with one molecule in the center and others surrounding them.

Figure 4(c) shows the magic number and some typical global minimum structures at $R = 0.6$, $2CLJ_8$ now changes into a structure with two 2CLJ dimers perpendicular to each other at center and others surrounding them. $2CLJ_9$, $2CLJ_{11}$, $2CLJ_{12}$, and $2CLJ_{15}$ remain the same structures as those at $R = 0.5$, but $2CLJ_{11}$ becomes a particular stable structure. $2CLJ_{16}$ is also a particular stable structure and similar to the windmill structure just like $2CLJ_9$ and $2CLJ_{11}$, but with three

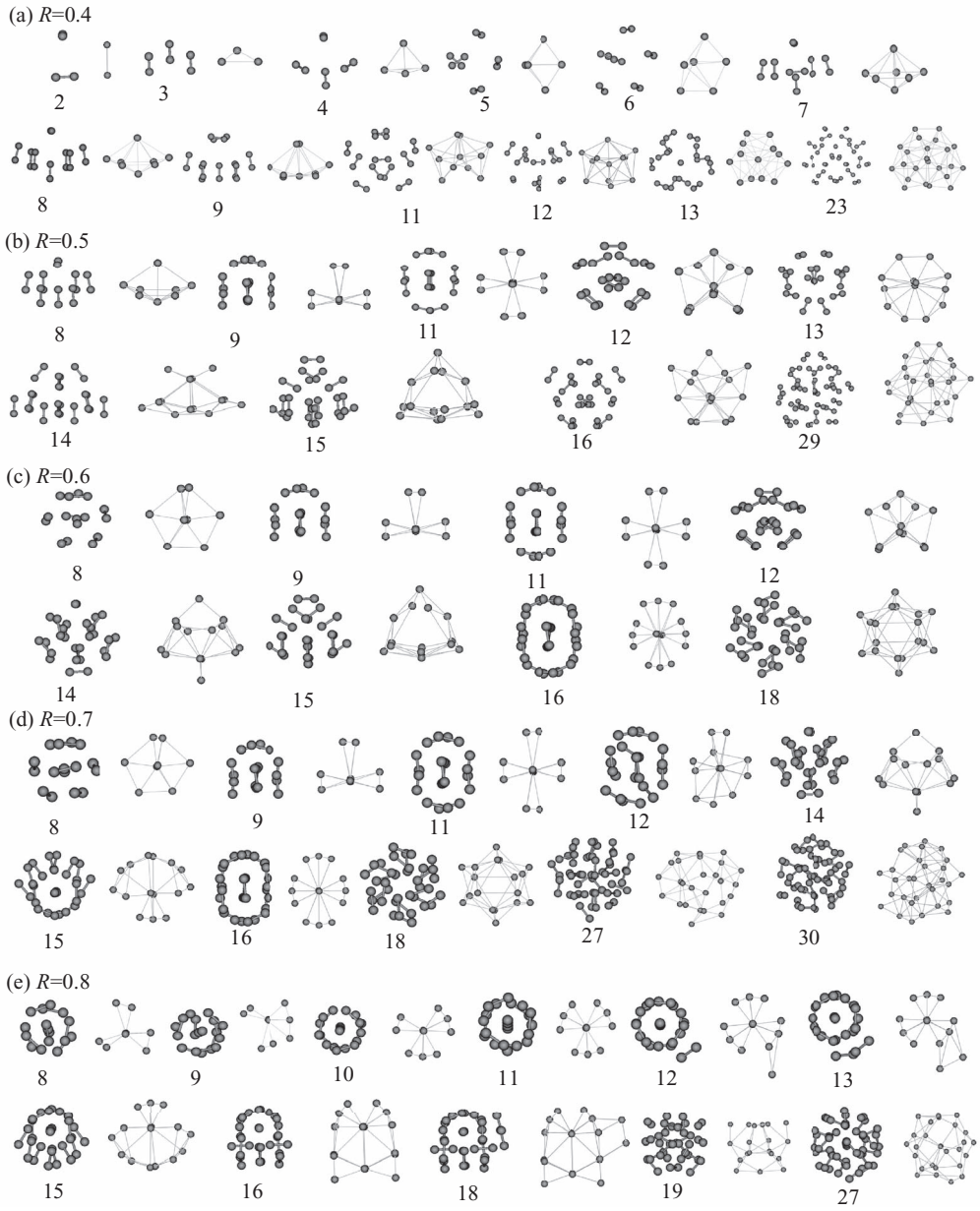

FIG. 4. Magic number and some typical global minimum structures of 2CLJ clusters at (a) $R = 0.4$, (b) $R = 0.5$, (c) $R = 0.6$, (d) $R = 0.7$, and (e) $R = 0.8$. For each cluster size, the structure on the left shows the real diatomic orientations, and that on the right shows an overall view of the cluster (each ball means the mass center of each molecule).

molecules per sail. $2CLJ_{14}$ and $2CLJ_{18}$ are with strange S_4 and S_6 symmetry, respectively.

Figure 4(d) shows the magic number and some typical global minimum structures at $R = 0.7$. $2CLJ_8$, $2CLJ_9$, $2CLJ_{11}$, $2CLJ_{14}$, $2CLJ_{16}$, and $2CLJ_{18}$ remain the same as those at $R = 0.6$. $2CLJ_{12}$ is based on $2CLJ_{11}$. $2CLJ_{15}$ is just like a mushroom. $2CLJ_{27}$ and $2CLJ_{30}$ are particular stable structures.

Figure 4(e) shows the magic number and some typical global minimum structures at $R = 0.8$. $2CLJ_{8–13}$ has the similar windmill structure. Two 2CLJ dimers at center in $2CLJ_8$ and $2CLJ_9$ are perpendicular to each other, but in $2CLJ_{10–13}$, they are positioned in a head-to-head manner, which is also different from the windmill structure at other R values. $2CLJ_{11}$ now is a windmill structure with three sails at 60° angle. $2CLJ_{12}$ and $2CLJ_{13}$ are based on $2CLJ_{11}$. $2CLJ_{15}$ is the same as it at $R = 0.7$. $2CLJ_{16}$ is with S_4 symmetry and $2CLJ_{18}$ is based on $2CLJ_{16}$. $2CLJ_{19}$ and $2CLJ_{27}$ are particular stable structures and $2CLJ_{19}$ is with C_2 symmetry. It is seen that with R increasing, this windmill structure becomes especially stable.

C. Anisotropy effect of 2CLJ dimer on pair potential range

With R increasing, the packing styles of 2CLJ clusters change greatly due to the anisotropy effect. For $2CLJ_{13}$, its structure changes from icosahedron to distorted icosahedron and to irregular motifs (Figs. 2 and 4). In order to clarify the anisotropy effect on the global minimum structures of

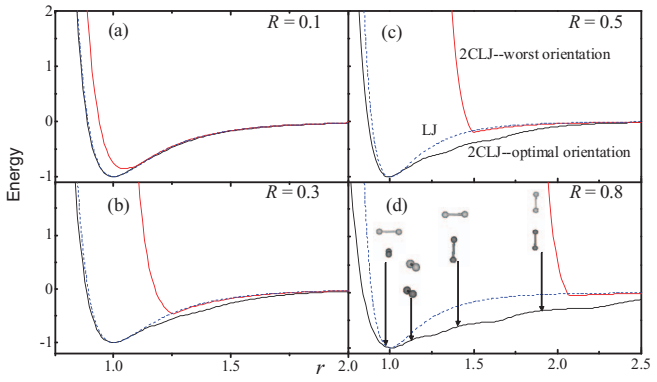

FIG. 5. The energy of $2CLJ_2$ potential at the optimal orientation and the worst orientation (as labeled) at (a) $R = 0.1$, (b) $R = 0.3$, (c) $R = 0.5$, and (d) $R = 0.8$. The LJ potential (dashed line) is also plotted for comparison. r is the distance of the mass center of the two 2CLJ dimer. For $R = 0.8$, structures of optimal orientation at $r = 0.9$, 1.1, 1.4, and 1.9 are labeled.

2CLJ clusters, at different R, we fix the distance between mass centers of two dimers to optimize the dimer orientation, and then we get the optimal orientation and the worst orientation. The potential energy curves of $2CLJ_2$ at the optimal orientation and at the worst orientation are plotted in Fig. 5 for $R = 0.1$, 0.3, 0.5, and 0.8, respectively, in which the LJ potential is also plotted for comparison. It is seen that at $R = 0.1$, the $2CLJ_2$ potential curve at the optimal orientation is very close to the LJ potential curve, and their structures are also similar. For the optimal orientation, with R increasing (increase of anisotropy effect), the short-range interaction between two diatomic molecules becomes softer and the long-range interaction becomes stronger, so the potential range increases. However, at the worst orientation, the potential range decreases with R increasing. Besides, the energy difference at the optimal and worst orientation also increases with R. Therefore, it is seen that increasing the anisotropy effectively softens the potential at optimal orientation, which leads to the global minima of 2CLJ clusters changing from icosahedral, to polyicosahedral and to novel irregular structures.

This kind of softness resulting from anisotropy effect for 2CLJ potential is similar to that of Morse potential[28] with potential parameters changing. It is seen that as the potential softens for 2CLJ and Morse clusters,[25,29,30] the decahedral and close-packed structures are not favored any longer for both of them, but icosahedral and disordered structures are favored. There is also some difference in the morphologies of the 2CLJ and Morse clusters. At small R with small anisotropy effect, $2CLJ_{34}$ is a distorted Leary tetrahedral, which is not the optimal structure for Morse potential, but for modified Morse potential.[31,32] Moreover, due to the anisotropy effect, all packings (icosahedral, decahedral, close-packed) are seriously strained for 2CLJ clusters. Hence, different to Morse clusters, the six-fold polyicosahedral packing is more favored for 2CLJ clusters due to its large number of nearest neighbors. As anisotropy effect increases, for 2CLJ potential at $R = 0.4$–0.8, some novel and disordered structures are favored, different from any known packing for Morse and LJ clusters.

It is noted that the potential energy curves in Fig. 5 show some small degree of oscillation. The oscillation mainly derives from the change of molecular orientation of $2CLJ_2$. In Fig. 5, structures of optimal orientation at $r = 0.9$, 1.1, 1.4, and 1.9 are also listed, which reveals that, with distance increase, the optimal orientation of two 2CLJ dimers varies from cross-shape, shoulder-to-shoulder, T-shape, and head-to-head geometry.

IV. CONCLUSIONS

The global minimum structures of 2CLJ clusters are located using the funnel hopping algorithm, in which anisotropic parameter (the ratio of the diatomic bond length to the LJ equilibrium length) is varied from 0.1 to 0.8 (step size is 0.1). Compared to LJ atomic clusters model, the structures of 2CLJ model are anisotropic. All packings (icosahedral, decahedral, and polyicosahedral) are seriously strained, so the six-fold polyicosahedral packing is favored due to its large number of nearest neighbors at $R = 0.1$–0.3. With the increase of anisotropy effect, the potential range increases at optimal orientation, and the global minima change from icosahedral, to polyicosahedral and to novel irregular structures. Compared with LJ and 2CLJ at $R = 0.1$–0.3 whose global minimum structures are regular, the most favored motifs of 2CLJ clusters at $R = 0.4$–0.8 are irregular and novel, some of which are interesting, such as windmill-shape or mushroom-shape. 2CLJ model is the simplest, but it can clearly demonstrate the anisotropy effect on the structures of diatomic clusters. It is expected to provide a good indicator to those anisotropic systems in a real physical world.

ACKNOWLEDGMENTS

This work is supported by the National Natural Science Foundation of China (NNSFC) (20903001) and by the 211 Project of Anhui University.

[1] F. Baletto and R. Ferrando, Rev. Mod. Phys. **77**, 371 (2005).
[2] A. M. Bittner, Surf. Sci. Rep. **61**, 383 (2006).
[3] S. Ogut, J. C. Idrobo, J. Jellinek, and J. L. Wang, J. Cluster Sci. **17**, 609 (2006).
[4] E. G. Noya and J. P. K. Doye, J. Chem. Phys. **124**, 6 (2006).
[5] W. S. Cai, Y. Feng, X. G. Shao, and Z. X. Pan, J. Mol. Struct.: THEOCHEM **579**, 229 (2002).
[6] J. E. Lennard-Jones, Proc. R. Soc. London, Ser. A **109**, 584 (1925).
[7] D. J. Wales and J. P. K. Doye, J. Phys. Chem. A **101**, 5111 (1997).
[8] X. L. Yang, W. S. Cai, and X. G. Shao, J. Comput. Chem. **28**, 1427 (2007).
[9] D. J. Wales, J. P. K. Doye, A. Dullweber, M. P. Hodges, F. Y. Nakamura, F. Calvo, J. Hernández-Rojas, and T. F. Middleton, The Cambridge Cluster Database (CCD); see http://www-wales.ch.cam.ac.uk/CCD.html.
[10] D. Sabo, J. D. Doll, and D. L. Freeman, J. Chem. Phys. **121**, 847 (2004).
[11] D. Sabo, C. Predescu, J. D. Doll, and D. L. Freeman, J. Chem. Phys. **121**, 856 (2004).
[12] J. P. K. Doye and L. Meyer, Phys. Rev. Lett. **95**, 4 (2005).
[13] J. P. K. Doye, A. Dullweber, and D. J. Wales, Chem. Phys. Lett. **269**, 408 (1997).
[14] L. J. Cheng, W. S. Cai, and X. G. Shao, ChemPhysChem **6**, 261 (2005).
[15] J. P. K. Doye, D. J. Wales, W. Branz, and F. Calvo, Phys. Rev. B **64**, 235409 (2001).
[16] L. Cheng, Y. Feng, and J. Yang, J. Chem. Phys. **130**, 214112 (2009).
[17] I. Napari and A. Laaksonen, J. Chem. Phys. **126**, 134503 (2007).
[18] D. C. Liu and J. Nocedal, Math. Program. **45**, 503 (1989).
[19] D. M. Deaven and K. M. Ho, Phys. Rev. Lett. **75**, 288 (1995).
[20] R. L. Johnston, Dalton Trans. **22**, 4193 (2003).
[21] B. Hartke, J. Comput. Chem. **20**, 1752 (1999).

[22]X. G. Shao, L. J. Cheng, and W. S. Cai, J. Comput. Chem. **25**, 1693 (2004).
[23]E. Yurtsever, F. Calvo, and D. J. Wales, Phys. Rev. E **72**, 10 (2005).
[24]R. H. Leary and J. P. K. Doye, Phys. Rev. E **60**, 6320 (1999).
[25]L. J. Cheng and J. L. Yang, J. Phys. Chem. A **111**, 5287 (2007).
[26]J. Wu and L. J. Cheng, J. Chem. Phys. **134**, 194108 (2011).
[27]J. P. K. Doye, D. J. Wales, and R. S. Berry, J. Chem. Phys. **103**, 4234 (1995).
[28]P. M. Morse, Phys. Rev. **34**, 57 (1929).
[29]Y. Feng, L. J. Cheng, and H. Y. Liu, J. Phys. Chem. A **113**, 13651 (2009).
[30]J. P. K. Doye and D. J. Wales, J. Chem. Soc., Faraday Trans. **93**, 4233 (1997).
[31]J. Wu and L. J. Cheng, J. Chem. Phys. **134**, 194108 (2011).
[32]L. J. Cheng and J. L. Yang, J. Chem. Phys. **127**, 124104 (2007).